



ADSORPTION OF FUMARIC AND MALEIC ACIDS ONTO HYDROXYAPATITE: A THERMODYNAMIC STUDY

Enrique D. Vega¹♥ and Pedro A. Colinas²

¹Area de Química General e Inorgánica "Dr. Gabino F. Puelles", Facultad de Química, Bioquímica y Farmacia. Universidad Nacional de San Luis. Chacabuco 917. (5700) San Luis, Argentina.

²LADECOR, Departamento de Química. Facultad de Ciencias Exactas. Universidad Nacional de La Plata. 47 y 115 (1900) La Plata, Argentina.

Received February 2, 2010. In final form July 6, 2010.

Abstract

The interaction of fumaric and maleic acids in aqueous solution with synthetic hydroxyapatite has been studied. Maleic and fumaric acids are found to be adsorbed to hydroxyapatite via the completely deprotonated carboxylates. Maleic acid shows the strongest adsorption due to its *cis* geometry. The adsorption isotherms fit the Langmuirian shape. The maximum adsorption is observed at pH 4.1 for fumaric acid and pH 5.2 for maleic acid. HAP should be useful to selective removal of fumaric and maleic acids from wastewaters.

Keywords: hydroxyapatite; fumaric acid; maleic acid; isotherms; solid-liquid interactions

♥Corresponding author. E mail: evega@unsl.edu.ar FAX: +54 2652 430224

Resumen

En este trabajo se reportan datos termodinámicos para la adsorción de los ácidos fumárico y maleico sobre hidroxiapatita. Ambos ácidos se adsorben en la superficie de hidroxiapatita como carboxilatos. El ácido maleico se adsorbe considerablemente debido a su geometría cis. Las isotermas muestran comportamiento tipo Langmuir. La máxima adsorción tiene lugar a pH 4,1 para ácido fumárico y a pH 5,2 para ácido maleico. El empleo de hidroxiapatita resulta promisorio para la remoción de los ácidos de aguas residuales.

Palabras clave: hidroxiapatita; ácido fumárico; ácido maleico; isotermas; interacciones sólido-líquido

Introduction

Fumaric and maleic acids arise as waste products from certain industrial processes, such as manufacture of maleic or phthalic anhydrides and catalytic oxidation of aromatic compounds [1,2]. Recently it has been showed that electrochemical oxidation of phenols is an useful methodology to decontaminate wastewaters. Among others, fumaric and maleic acids are end products of the oxidation [3,4]. As the environmental protection is getting increasing attention, it is useful to find an efficient and low cost method to remove fumaric and maleic acids from industrial wastewaters. Much research has been done to treat fumaric acid wastewater, including microelectrolysis of iron and carbon, catalytic microwave oxidation, peroxide oxidation, bio-contact oxidation, anaerobic hydrolysis, complex extraction and reverse osmosis [5]. Although they are useful methods, acids are degraded and cannot be recovered in most of them. Therefore, the adsorption of fumaric and maleic acids on different materials could be a suitable solution to this problem. Several studies have evaluated the adsorption characteristics of these acids. Dobson and McQuillan, for example, examined the adsorption of maleic and fumaric acids, between other dicarboxylic acids, to four metal oxides (TiO_2 , ZrO_2 , Al_2O_3 , and Ta_2O_5) [6]. Later on, adsorption to gibbsite [7] and hematite [8] was analyzed. These studies did not agree on the controlling adsorption mechanisms and structure of the adsorbed compounds.

Hydroxyapatite [$\text{Ca}_{10}(\text{PO}_4)_6(\text{OH})_2$, HAP] is the main component of hard tissues of vertebrates such as bones and teeth. It has a strong ability to fix heavy metals and has been applied for purification of wastewaters [9-13] and soil remediation [14-17]. In previous works [18-22] we studied the adsorption of VO^{2+} ions and citric acid onto carbonateapatite and crystalline HAP.

In all cases the adsorbed amounts depend of several aspects, such as the characteristics of the functional groups, molecular structure and the size of the adsorbates, the nature of the surface and the composition of the aqueous phase. For anions, it has been observed that the maximum of adsorption takes place at pH values in the surroundings of their pK_a [23,24].

The purpose of the present work is to explore the use of HAP in treatment of industrial effluents to evaluate its ability for the removal of fumaric and maleic acids from aqueous solutions. HAP was chosen among other possible adsorbents because of its high availability and "a priori" satisfactory sorptive properties. In this paper we present the main characterization data for the solid used as adsorbent and the study of its interaction with fumaric and maleic acids through batch experiments in aqueous solutions in the range of temperatures 278-308 K. The Langmuir parameters for the adsorption phenomenon are calculated and the capacity of the uptake is evaluated.

Experimental**Materials**

Reagents of analytical grade were used in the synthesis of HAP according to the following procedure. Microcrystalline powder was obtained by precipitation in a discontinuous reactor as

described by Hayek and Stadlmann [25]. The method, that involves the reaction of equimolar quantities of solutions of $\text{Ca}(\text{NO}_3)_2 \cdot 4\text{H}_2\text{O}$ and $\text{NH}_4\text{H}_2\text{PO}_4$ at $\text{pH}=12$, was chosen because large batches of product can be obtained. The dried solid was calcined at 1073 K for 2 hours. HAP was obtained as white, well-crystallized powder.

Fumaric (BDH) and maleic (Riedel de Haen) acids are commercially available.

Characterization of materials

Scanning electron microscopy (SEM) technique was used to observe and analyze the morphology and the particle size of the pure HAP powders. Samples were placed on an adhesive carbon tape coated with gold and observed in a LEO1450VP. Energy dispersive X-ray spectroscopy (EDS) was performed for chemical microanalysis using an EDAX system.

The characterization of HAP was also carried out by X-ray diffraction (XRD) measurements. X-ray powder diagrams were obtained with a Rigaku D-MAX-IIIC diffractometer using CuK_α radiation (Ni-filter) and NaCl and quartz as external calibration standards.

Chemical composition was determined by inductively coupled plasma spectroscopy in an atomic emission spectrometer associated to an inductively coupled plasma Baird ICP 2070.

The specific surface area, S_g , (by N_2 adsorption-desorption method at 77 K) was determined with a Micromeritics Accusorb 2100E for an outgassing time of 14 h.

Fumaric acid was repeatedly crystallized from water until constant melting point (290-291°C). Maleic acid was crystallized from acetone/hexane (m.p. 142-143°C). The acids were dried *in vacuo* in the presence of phosphorous pentoxide [26]. The purity of compounds was confirmed by IR, ^1H and ^{13}C NMR spectroscopy.

Fumaric and maleic acids concentrations were determined by UV-Visible spectrometry in a Shimadzu UV-160A recording spectrophotometer.

Adsorption Experiments

The experimental data for the fumaric and maleic acids adsorption on the surface of synthetic HAP were obtained in a batch system consisting of an erlenmeyer flask with a magnetic stirring bar inside to mix the solution. The flask was partially immersed in a bath at 288, 298 or 308 K to maintain constant temperature. Experiments were carried out by contacting 1 g of HAP with 50 mL of acidic solution with a known initial concentration in the range of 3 to 200 mg L^{-1} for 1 hour.

Determination of the adsorbed concentration

The extent of the adsorption for both acids was determined in the remnant solution after filtration once each batch experiment was over. The concentration of the adsorbates was determined from their absorbances at 210 nm for fumaric acid and at 204 nm for maleic acid. Measurements of adsorbed acids were made on the solid residue to corroborate the absence of errors. They showed an excellent agree with those made in the remaining solutions.

Results and discussion

Characteristics of HAP

According to the SEM observation (Figure 1), the synthesized HAP particles are spherical-shaped with radius sizes ranging 120 nm and 180 nm.

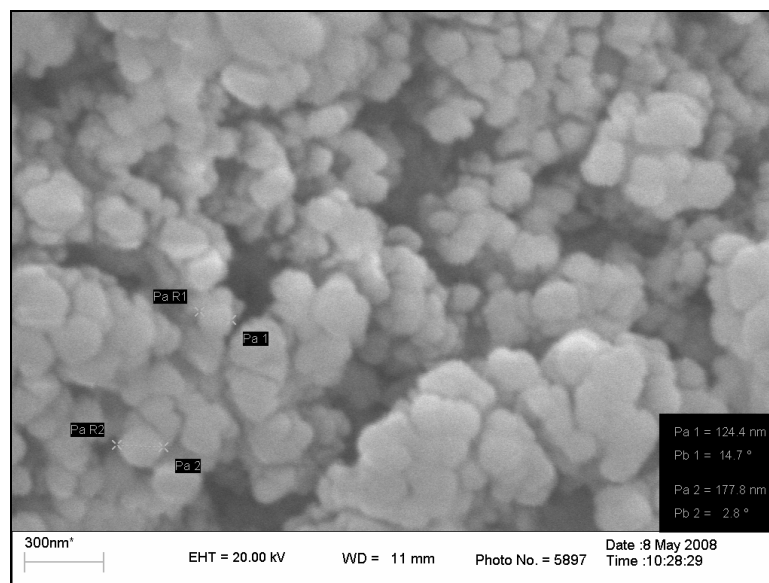


Figure 1. Scanning electron micrograph of HAP.

The mineralogical identity of HAP particles was verified by XRD analysis. The cell parameters of the hexagonal lattice ($a = 9.41 \text{ \AA}$ and $c = 6.87 \text{ \AA}$) are in agreement with those of JCPDS 9-432 [27]. Figure 2 shows the XRD pattern of crystalline HAP. The well-defined diffraction peaks account for the high crystallinity of the sample.

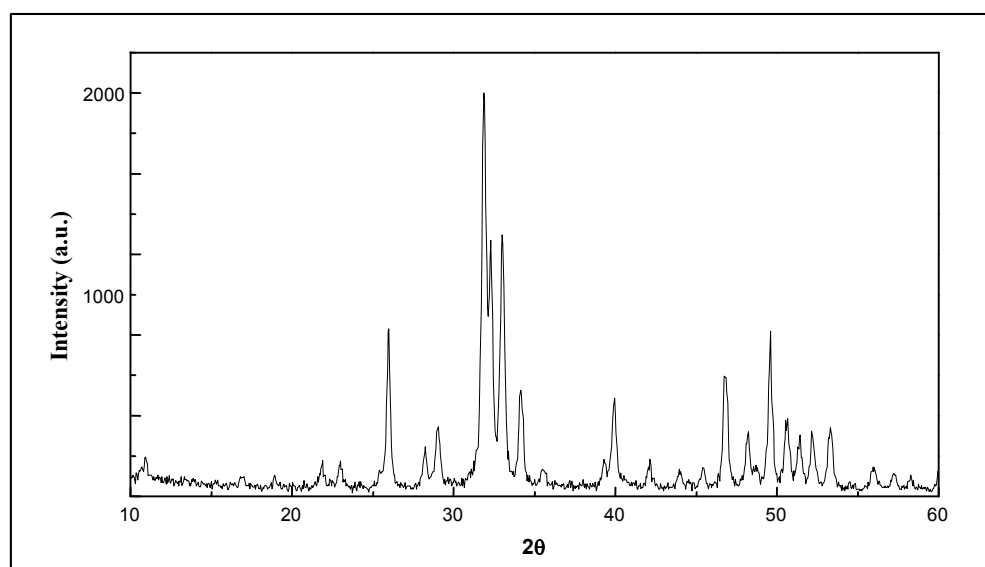


Figure 2. XRD pattern of crystalline HAP.

The Ca/P ratio is 1.61, as against the ratio 1.67 for the stoichiometric HAP. The specific surface area, determined by the BET method, was $18 \text{ m}^2 \text{ g}^{-1}$.

Adsorption kinetics of fumaric and maleic acids onto HAP

Adsorption kinetics curves of fumaric and maleic acids onto HAP at pH 4.5 and initial concentrations 10^{-4} mol L⁻¹ are shown in Figure 3, where the amount of adsorbed acids ($\Gamma/\mu\text{mol g}^{-1}$) against time is reported. The kinetic curves reveal a rapid adsorption of both acids to reach equilibrium at 35 min of contact and remain in equilibrium for additional periods of contact. The system was kept 1 h to ensure equilibrium in the isothermic assays.

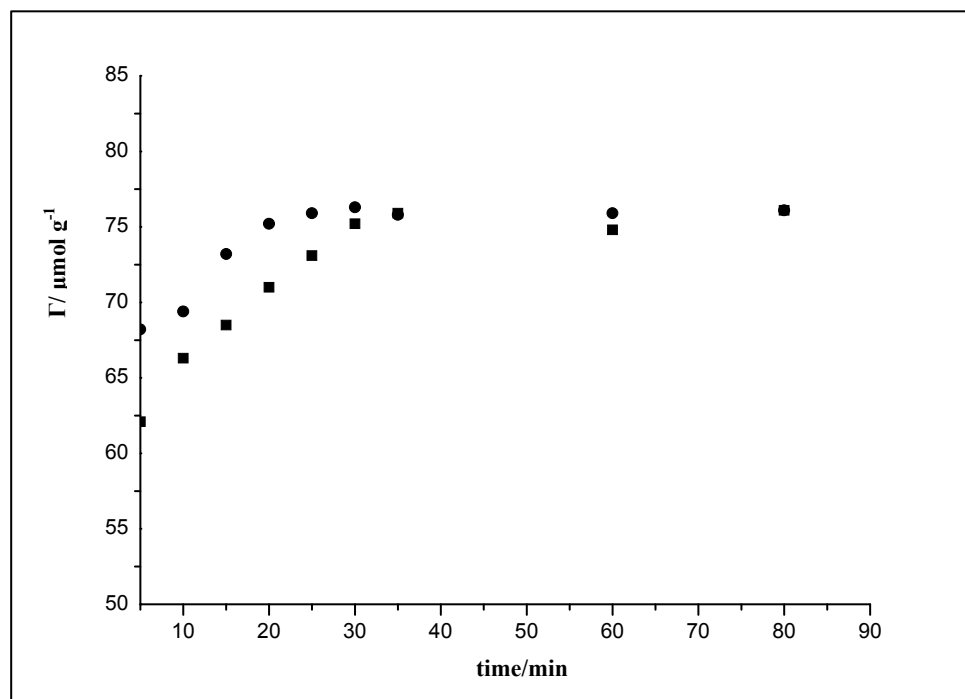


Figure 3. Extent of the adsorption against time for the systems HAP-fumaric acid (■) and HAP-maleic acid (●).

pH dependence

The pH effect has been analyzed as it is one of the most important factors to study the adsorption of ions on solids. The pH can substantially affect the surface electric charge of the adsorbent which is important for the electrostatic interaction of ions.

Otherwise, the protonation-deprotonation of the acids is conditioned on pH according their pK_a values (see Figure 4).

At low pH values adsorption is negligible whereas an increment in a few units produces an important increase in the adsorbed amounts.

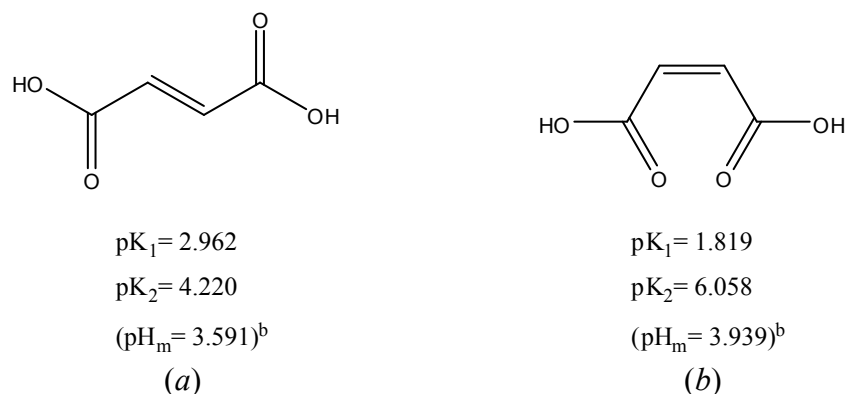


Figure 4. pK_a values for fumaric (a) and maleic (b) acids. $(pH_m)^b = pK_1 + \frac{1}{2}(pK_2 - pK_1)$.

Figure 5 shows the experimental data obtained in the study of the pH influence in the adsorption for fumaric and maleic acids onto HAP in the range pH 3 to 6.6.

It can be observed that maximum adsorption takes place at pH values 4.1 for fumaric acid and 5.2 for maleic acid. Taking into account this experimental data, it can be seen that the maximum adsorption occurs at pH values in the neighbouring of their second ionization constants in both cases. This fact implies that mono- and dicarboxylate ions are present. The increase dicarboxylic/monocarboxylic ratio partially affects the adsorption of maleic acid whereas it produces a remarkable diminution for fumaric acid.

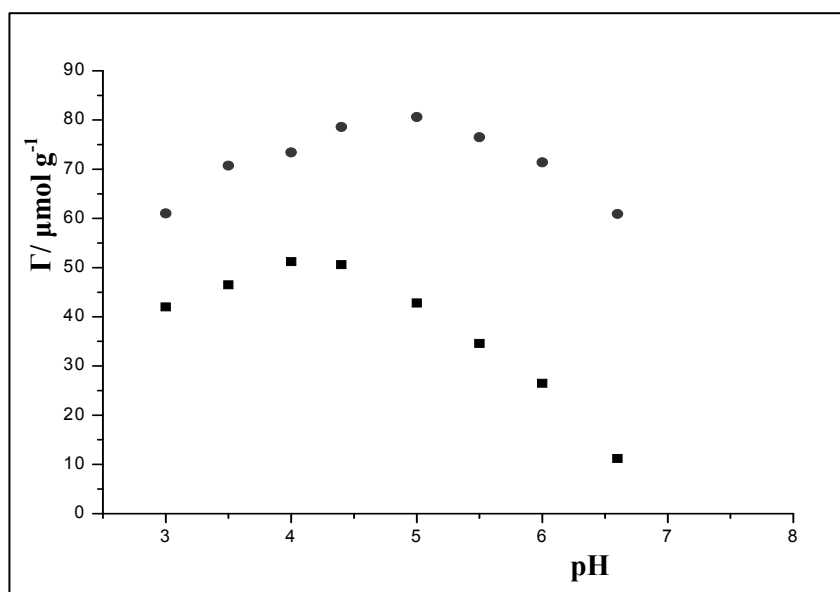


Figure 5. pH dependence for the adsorption of fumaric and maleic acids onto HAP: (■) fumaric acid; (●) maleic acid.

Adsorption isotherms of fumaric and maleic acids onto HAP

The Langmuir absorption model [28] considers the following assumptions: (i) the adsorption sites are isoenergetic, (ii) only a monolayer of adsorbate is formed, and (iii) there are no interactions between the adsorbate molecules either in the solution or on the surface of the adsorbent.

Taking into account the structural and reactive features of the adsorbent and both adsorbates, it is evident that the three Langmuir assumptions cannot be applied to the present systems. In particular, all the active regions of HAP are not equivalent and its surface is not uniform. Otherwise, the ability of fumaric and maleic acids to be adsorbed at a given site is dependent on the occupation of neighbouring sites because of the steric factor present in these cases.

Nevertheless, it is well known that the Langmuir equations are useful in explaining the adsorption of nonelectrolytes from highly diluted solutions, which resembles the adsorption of gases by solid adsorbents.

However, it can be seen that, under the experimental conditions mentioned above, the data for adsorptive uptake of fumaric and maleic acids from aqueous solutions by HAP show Langmuir-type isotherms, but do not fit the Langmuir model.

Consequently, a modified expression for the Langmuir equation, previously used by Vega et al. [21] to explain the adsorption of citric acid onto HAP may be used to explain experimental data:

$$C_a = \frac{K_{ad} L C^{0.5}}{(1 + K_{ad} C^{0.5})} \quad [1]$$

The above equation is equivalent to the linear expression,

$$\frac{C^{0.5}}{C_a} = \frac{1}{(L K_{ad}^{0.5})} + \frac{1}{L} C^{0.5} \quad [2]$$

where K_{ad} stands for the equilibrium constant of the adsorption reaction, and L represents the total number of active sites per gram of adsorbent. From the linear $\frac{C^{0.5}}{C_a}$ plot vs. $C^{0.5}$ the constants K_{ad} and L can be calculated.

Adsorption isotherms of fumaric and maleic acids onto HAP at different temperatures and initial concentrations 10^{-3} to 10^{-4} mol L⁻¹ are shown in Figures 6 and 7, respectively. The amounts of adsorbed acids increased with the increase of acid concentrations in the equilibrium solution. The reaction mechanism for the adsorption of both acids includes their surface complexation with HAP. Figures 8 and 9 show the plot of the linear Eq (2) for both acids at the three temperatures of work. The excellent correlation coefficients for these linear equations constitute a good support for the proposed adsorption isotherm.

The obtained values for K_{ad} and L are reported in Table 1.

Table 1. Adsorption of fumaric and maleic acids by HAP. Value of the constants that characterize the adsorption isotherm proposed Eq. (2).

	Fumaric Acid			Maleic Acid		
T (K)	288	298	308	288	298	308
$L \times 10^{-19}$ (mol g ⁻¹)	5.97	4.76	4.53	8.79	5.72	3.41
K_{ad} $L^{0.5} \text{ mol}^{-0.5}$	30.66	26.92	21.15	36.2	33.41	28.9
r	0.9966	0.9971	0.9946	0.9980	0.9979	0.9967

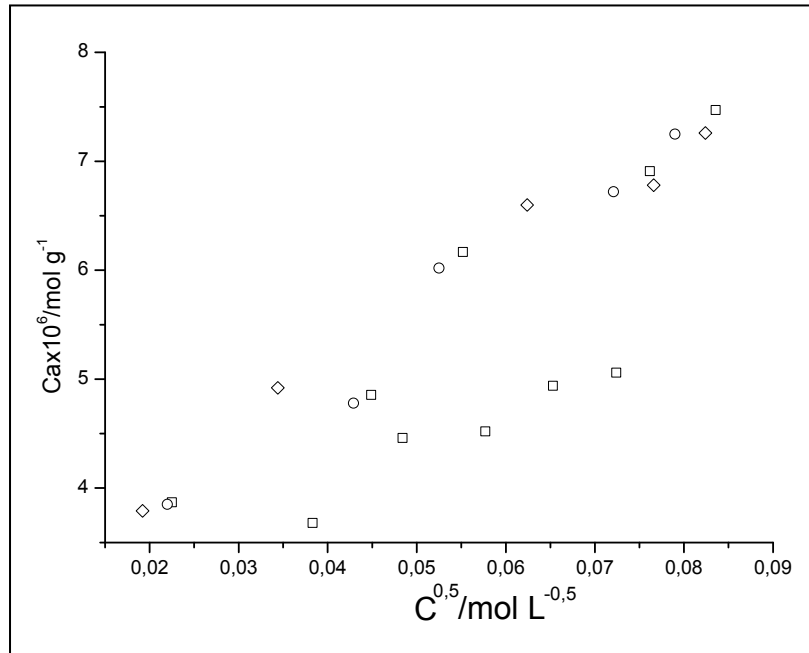


Figure 6. Adsorption isotherms of fumaric acid by hydroxyapatite from dilute solutions at (\diamond) 288, (\circ) 298 and (\square) 308 K.

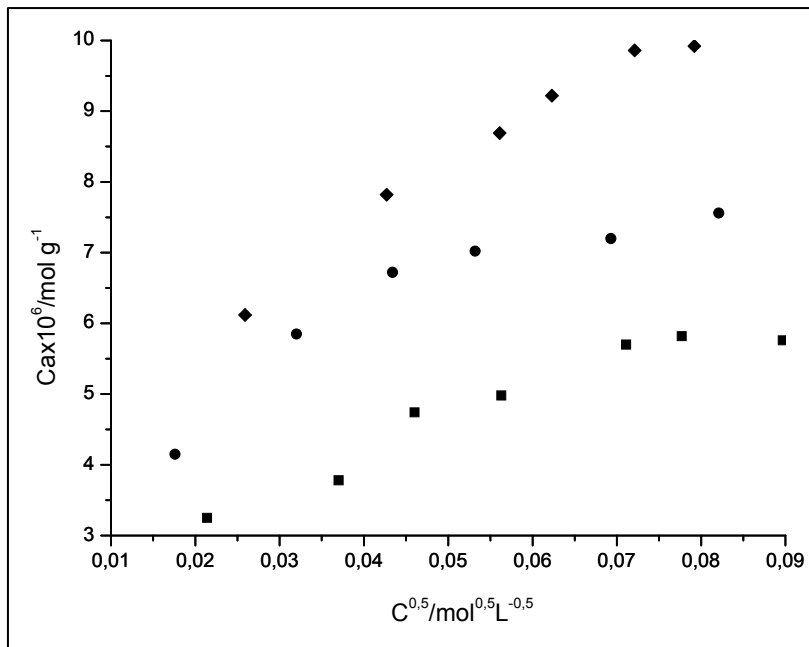


Figure 7. Adsorption isotherms of maleic acid by hydroxyapatite from dilute solutions at (\blacklozenge) 288, (\bullet) 298 and (\blacksquare) 308 K.

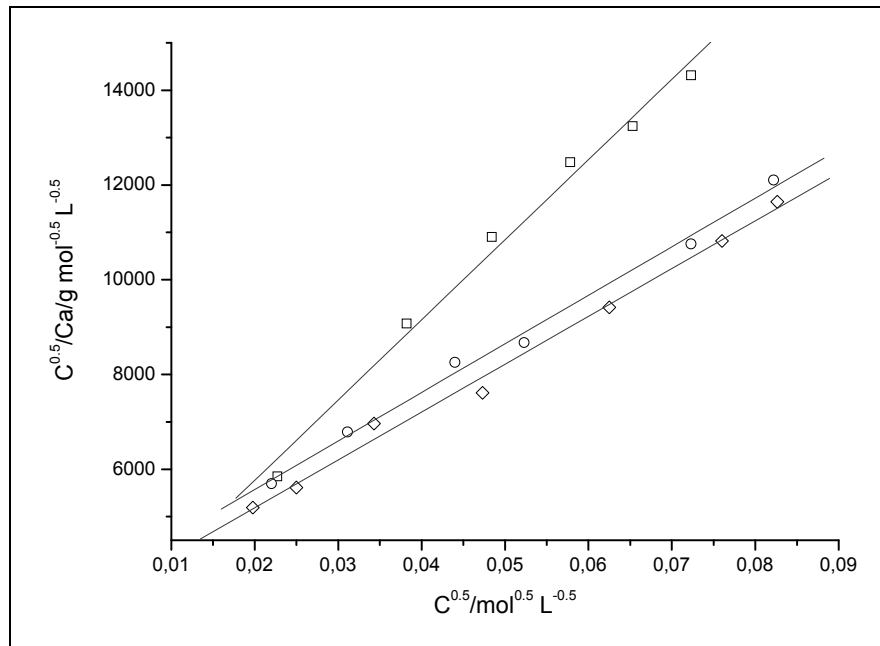


Figure 8. Adsorption isotherms of fumaric acid by hydroxyapatite from dilute solutions. Plot of the linear equation, Eq. (2). (\diamond) 288, (\circ) 298 and (\square) 308 K.

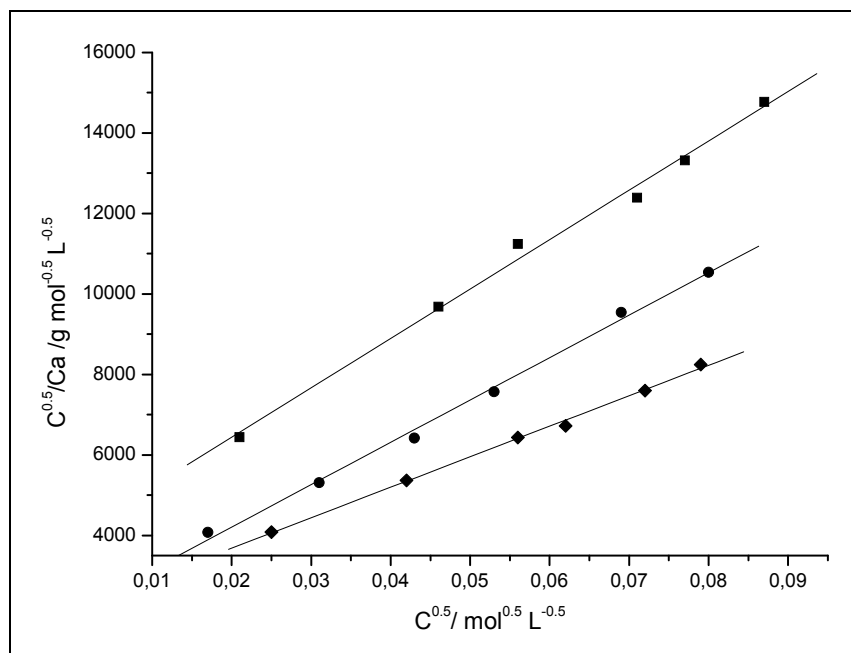


Figure 9. Adsorption isotherms of maleic acid by hydroxyapatite from dilute solutions. Plot of the linear equation, Eq. (2). (\diamond) 288, (\bullet) 298 and (\blacksquare) 308 K.

From Table 1, it can be observed that, in both cases, K_{ad} decreases when the absolute temperature (T) of the medium increases. This fact indicates that the formation of the surface complex implies a typical exothermic reaction.

To obtain the thermodynamic magnitudes ΔH_r° (standard heat of reaction) and ΔS_r° (standard entropy of reaction) which characterize the adsorption process the van't Hoff equation was used (see Figure 10). Table 2 displays the obtained thermodynamic values.

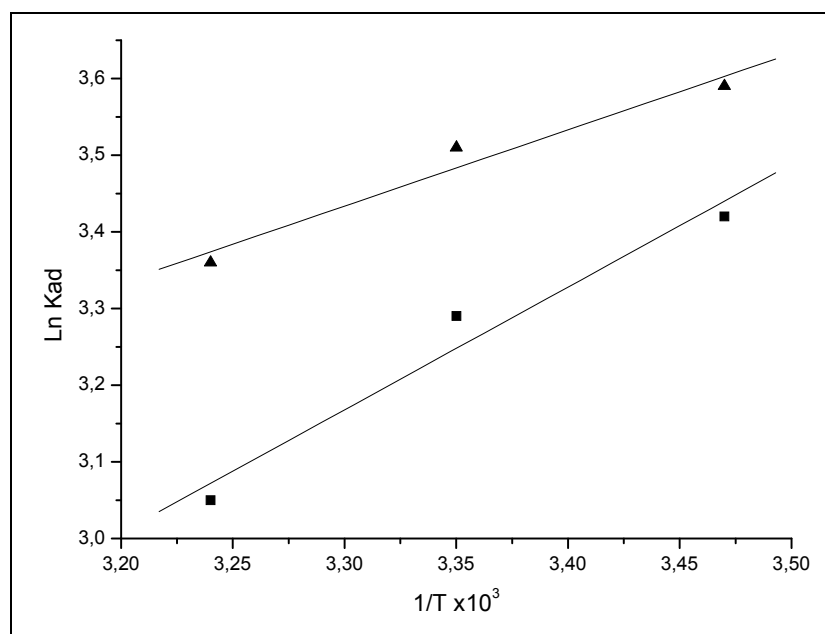


Figure 10. Determination of the standard heat and standard entropy for the adsorption reaction between fumaric acid (■) and maleic acid (▲) and HAP by means of the van't Hoff equation.

Table 2. Adsorption of fumaric and maleic acids by HAP. Value the thermodynamic magnitudes ΔH_r° (standard heat of reaction) and ΔS_r° (standard entropy of reaction) which characterize corresponding the adsorption process.

	Fumaric Acid	Maleic Acid
$\Delta H_r^\circ / \text{Kcal mol}^{-1}$	-3.16	-1.15
$\Delta S_r^\circ / \text{cal mol}^{-1}\text{K}^{-1}$	-4.17	-2.98

It can be clearly observed that the increase of the temperature values in the reacting medium tends to avoid the occurrence of both studied adsorption reactions.

Conclusions

In this paper, we have demonstrated the possibility of explaining the adsorption of fumaric and maleic acids by hydroxyapatite from aqueous solutions alter a model that involves an association complex that includes the adsorbate and the adsorbent. Maximum adsorption takes place at 35 minutes of contact and at pH 4.1 for fumaric acid and pH 5.2 for maleic acid.

Fumaric and maleic acids are almost exclusively adsorbed as dicarboxylates. The strong adsorption of maleic acid could be explained in terms of surface coordination *via* bridging bidentate carboxylate groups. This result is not unexpected, as the *cis* conformation of maleic acid should provide an ideal orientation for coordination *via* both carboxylate groups. Due to the *trans* orientation of fumaric acid, it may not be expected to readily adsorb at HAP surface.

A modified Langmuir adsorption isotherm fits the experimental data very satisfactorily. The thermodynamic magnitudes associated with the adsorption process, ΔH_r° and ΔS_r° , reported here, allowed us to conclude that the proposed model is adequate to our purpose. The obtained values for the standard heat of adsorption indicate that adsorption reactions are exothermic processes and their magnitudes indicate that physisorption phenomena occur. Otherwise, the calculated standard entropies of adsorption are coherent with this kind of processes.

The batch experimental data related to the interaction of fumaric and maleic acids with hydroxyapatite are promising for an eventual use of this adsorbent in decontamination of liquid industrial wastes in pre-diluted samples or as a second step in a combined process.

Acknowledgements. We thank the financial support of ANPCyT (Project PICT 25459), SECyT-UNSL (Project 7707) and CONICET (PIP 6246). The authors would like to thank Dr. María del Rosario Torres for the scanning electron micrographs. P. A. C. is member of CONICET.

References

- [1] M.J. Brackin, D.E. McKenzie, B.M. Hughes, M.A. Heitkamp, *Microbiology*, **1996**, *16*, 216.
- [2] C.K. Doscher, J.H. Kane, G.O. Cragwall, W.H. Staebner, *Ind. Eng. Chem.*, **1941**, *33*, 315.
- [3] M. Pimentel, N. Oturan, M. Dezotti, A. Mehmet, *Applied Catalysis B: Environmental*, **2008**, *83*, 140.
- [4] E. Brillas, M.A. Baños, M. Skoumal, P.L. Cabot, J.A. Garrido, R.M. Rodríguez, *Chemosphere*, **2007**, *68*, 199.
- [5] S. Li, J. Zhuang, T. Zhi, H. Chen, L. Zhang, *Desalination*, **2008**, *34*, 362.
- [6] K.D. Dobson, A.J. McQuillan, *Spectrochimica Acta - Part A: Molecular and Biomolecular Spectroscopy*, **1999**, *55*, 1395.
- [7] J. Rosenqvist, K. Axe, S. Sjöberg, P. Persson, *Colloids and Surfaces A: Physicochemical and Engineering Aspects*, **2003**, *220*, 91.
- [8] Y.S. Hwang, J.J. Lenhart, *Langmuir*, **2008**, *24*, 13934.
- [9] Q.Y. Ma, T.J. Traina, J.A. Logan, J.A. Ryan, *Environ. Sci. Technol.*, **1994**, *28*, 1219.
- [10] G. Lusvardi, G. Malavasi, L. Menabue, M. Saladini, *Waste Manag.*, **2002**, *22*, 853.
- [11] I. Smiciklas, S. Dimovic, I. Peclas, M. Mitric, *Water Res.*, **2006**, *40*, 2267.
- [12] S. Baille, A. Nzihou, D. Bernache-Assolant, E. Champion, P. Sharrock, *J. Hazard. Mater.*, **2007**, *139*, 443.
- [13] R.R. Sheha, *J. Colloid Interface Sci.*, **2007**, *310*, 18.
- [14] V. Laperche, S.J. Traina, P. Gaddam, T.J. Logan, *Environ. Sci. Technol.*, **1996**, *30*, 3321.
- [15] E. Mavropoulos, A.M. Rossi, A.M. Costa, C.A. Perez, J.C. Moreira, M. Saldanha, *Environ. Sci. Technol.*, **2002**, *36*, 1625.
- [16] C. Keller, M. Marchetti, L. Rossi, N. Lugon-moulin, *Plant. Soil*, **2005**, *276*, 69.
- [17] P.K. Chaturvedi, C.S. Seth, V. Misra, *Chemosphere*, **2006**, *64*, 1109.

- [18] G.E. Narda, E.D. Vega, J.C. Pedregosa, S. Etcheverry, E.J. Baran, *Z Naturforsch*, **1992**, *47*, 395.
- [19] E.D. Vega, J.C. Pedregosa, G.E. Narda, *J. Phys. Chem. Solids*, **1999**, *60*, 759.
- [20] E.D. Vega, J.C. Pedregosa, G.E. Narda, P.J. Morando, *Water Res.*, **2003**, *37*, 1776.
- [21] E.D. Vega, G.E. Narda, F.H. Ferretti, *J. Colloid Interface Sci.*, **2003**, *268*, 37.
- [22] E.D. Vega, J.C. Pedregosa, G.E. Narda, *J. Argent. Chem. Soc.*, **2009**, *97(1)*, 1.
- [23] H.L. Y ao, H.H. Yeh, *Langmuir*, **1996**, *12*, 2989.
- [24] K. Mesuere, W. Fish, *Environ. Sci. Technol.*, **1992**, *26*, 2365.
- [25] E. Hayek, W. Stadlmann, *Angew. Chem.*, **1955**, *67*, 327.
- [26] D.D. Perrin, W.L.F. Armarego, *Purification of Laboratory Chemicals*. 3rd ed. Pergamon Press, 1999.
- [27] JCPDS (International Centre for Diffraction Data) Card 9-432.
- [28] I. Langmuir, *J. Am. Chem. Soc.*, **1916**, *38*, 2221.